

Nanohole-Enhanced Raman Scattering

Alexandre G. Brolo,^{*,†} Erin Arctander,[†] Reuven Gordon,[‡] Brian Leathem,[§] and Karen L. Kavanagh[§]

Department of Chemistry, University of Victoria, P.O. Box 3065, Victoria, B.C., Canada, V8W 3V6, Department of Electrical and Computer Engineering, University of Victoria, P.O. Box 3055, Victoria, B.C., Canada, V8W 3P6, and Department of Physics, Simon Fraser University, 8888 University Drive, Burnaby, B.C., Canada, V5A 1S6

Received July 23, 2004; Revised Manuscript Received August 25, 2004

ABSTRACT

Periodic arrays of sub-wavelength apertures (nanoholes) in ultrathin Au films were used as substrates for enhanced-Raman spectroscopy in the optical range. Nanohole-enhanced (resonance) Raman scattering from oxazine 720 (oxa) adsorbed on arrays of different periodicities (distance between the center of the holes) was obtained. The overall Raman intensity of the adsorbed molecule was dependent on the periodicity of these arrays. The enhancement factor reached a maximum for the array that presented the largest transmission at the excitation wavelength of the laser. This shows that the enhancement of the Raman signal is provided by surface plasmon (SP) modes excited at the array of nanoholes. SP excitations lead to spatial localization of the electromagnetic fields in nanometric regions close to the surface. This field localization, allied to the unique vibrational signature of the Raman scattering and the simplified optical arrangement from the transmission optics, suggests that arrays of nanoholes should be useful for the fabrication of dense biochips for the detection of Raman-labeled analytes with high sensitivity and selectivity.

Surface plasmons (SP) are electromagnetic waves that propagate along a metal–dielectric interface.¹ The excitation of SP modes leads to a strong concentration of light at the surface on the sub-wavelength scale. Advances in nanofabrication allow the creation of organized structures that can take full advantage of this spatial localization. The periodic arrays of sub-wavelength apertures (nanoholes) in metallic thin films are among the most promising of these structures for applications in photonic circuits and light manipulation at the sub-wavelength range.^{2,3} The arrays of nanoholes enable an increase in the transmission of light by several orders of magnitude when the SP resonance condition is achieved.² This phenomenon is being explored for possible applications in several relevant fields, ranging from quantum information processing⁴ to nanolithography.⁵ In addition, it has been demonstrated that the polarization properties of the transmitted light can also be manipulated by tailoring the shape of the nanoholes.^{6,7} This level of control provides the basis for the development of sub-wavelength polarizers and switches, which are essential elements in useful nanophotonics architectures.

The main application of SPs in biochemical and biomedical sciences is in chemical sensing.⁸ Surface plasmon

resonance (SPR) is among the most used techniques for monitoring binding events in biological systems.⁹ Traditionally, an SPR measurement consists of the excitation of extended SP modes through prism coupling, using a reflection geometry (Kretschmann configuration). These angle-resolved SPR devices are sensitive to surface processes at the submonolayer level.¹⁰ Periodic arrays of nanoholes in thin gold films can also be used as SPR sensors that operate in transmission mode.¹¹ In this case, the surface processes are monitored by the shift in the wavelength of the maximum transmission due to molecular adsorption.¹¹ Although the SPR methods provide good sensitivity, they lack specificity at the molecular level because their principle of operation relies on the response of the SP resonances to changes in the refractive index at the metal–dielectric interface. Molecular specificity is a powerful advantage of SP-enhanced spectroscopic methods over the SPR technique for chemical and biochemical analysis.

Surface-enhanced Raman scattering (SERS) is the most commonly used of the SP-mediated molecular spectroscopic methods. SERS can be a very sensitive method capable of single-molecule detection.¹² Although SERS signals from a variety of substrates and nanostructures are routinely observed,^{12–15} this effect has not been previously reported from molecules adsorbed on periodic arrays of nanoholes. In contrast, examples of enhanced fluorescence and IR absorption from species adsorbed on this class of substrates can be found in the literature.^{16–18} In principle, the enhanced-

* Corresponding author. Telephone (250) 721-7167; FAX (250) 721-7147; e-mail agbrolo@uvic.ca.

[†] Department of Chemistry, University of Victoria.

[‡] Department of Electrical and Computer Engineering, University of Victoria.

[§] Department of Physics, Simon Fraser University.

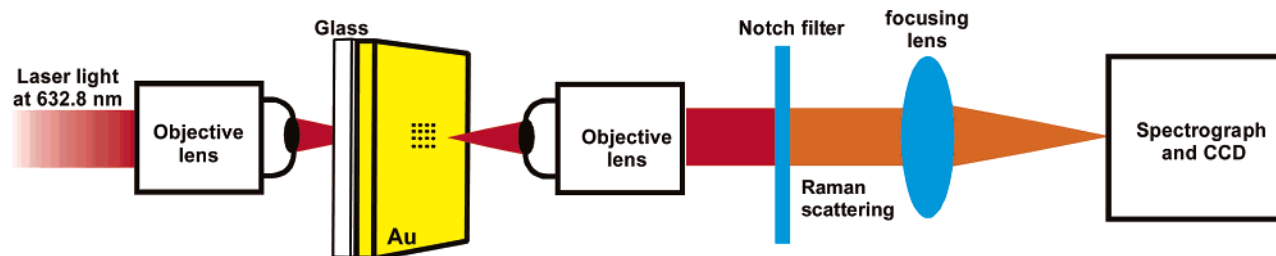


Figure 1. Experimental setup for transmission Raman spectroscopy through arrays of nanoholes. The excitation is shown from the glass–air interface. The analyte is adsorbed at the Au–air interface.

Raman has several advantages over these other spectroscopic methods. For instance, the bandwidth of the vibrational signature of the Raman signal is much narrower than the electronic fluorescence, providing a molecular fingerprint. Moreover, enhanced Raman scattering is obtained in the visible range, allowing simpler optics and better detection systems than IR absorption methods.

In this paper, the arrays of sub-wavelength holes in Au films were fabricated using focused ion beam (FIB) milling. The experimental parameters for the fabrication and cleaning of the substrates are given elsewhere.¹¹ Although silver and copper surfaces are known to produce better SERS, gold was used because it is easier to clean and much more stable chemically. The clean gold surface was modified by a droplet evaporation procedure. In this case, a drop of 10 μM solution of oxazine 720 (from Lambdachrome) in HPLC-grade methanol (Aldrich) was added to the surface. The solvent was allowed to evaporate, after which the surface was rinsed with a copious amount of ultrapure water (18.2 M Ωcm from a Barnstead NANOpure Diamond water purification system). This procedure ensured that at most one monolayer of the adsorbate was present at the surface during the Raman measurements.

Figure 1 shows the Raman instrumentation, which was modified from its conventional 90° arrangement to allow the spectral measurements to be made in transmission mode. This experimental geometry guarantees that the excitation photons at the gold–air interface were from the SP modes that were excited as part of the extraordinary transmission phenomenon. A 35 mW He–Ne laser (Melles Griot) was used as the excitation source, with a wavelength of excitation of 632.8 nm. The laser was directed from the glass side of the substrate and focused onto the array of nanoholes using a 10 \times Olympus microscope objective (numerical aperture = 0.25). The transmitted light (containing the Raman information) was collected using a similar microscope lens. The fundamental laser light was rejected using a Kaiser super-notch filter, and the remaining radiation was directed through a Kaiser Holospec f/1.4 spectrograph coupled with an Andor CCD detector (model DV-401-BV). The substrates and the lenses were mounted on mechanical stages that allowed fine positioning control, while a wide-view microscope was used to aid the alignment of the incoming laser light with the ca. 16 μm \times 16 μm arrays of nanoholes.

The chemical structure of oxazine 720 (oxa), a common laser dye with an absorption band at ca. 620 nm, is shown in the inset of Figure 2. The enhanced Raman spectra of

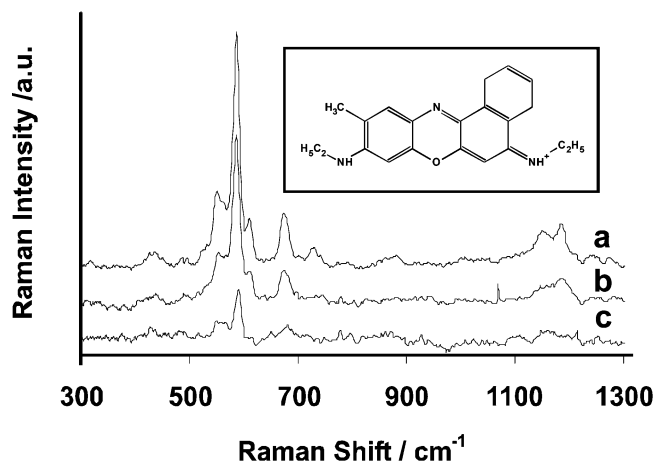


Figure 2. Enhanced Raman scattering from oxa adsorbed at the Au–air interface obtained using the setup shown in Figure 1. The spectra were obtained from arrays with different periodicities: (a) 560 nm; (b) 590 nm; (c) 620 nm. The spectra are offset for clarity.

oxa adsorbed on three arrays of nanoholes with different periodicities are shown in Figure 2a–c. The spectral features observed in Figure 2 are similar to the SERS of oxa adsorbed on a roughened silver electrode under electrochemical conditions.^{19,20} The main vibrational modes at 549, 585, 672, and 1181 cm^{-1} can all be assigned to the vibrations of the phenoxazine ring of the dye.²⁰ It is evident from Figure 2 that different degrees of enhancement of the Raman signal are observed for different arrays. This result can be correlated to the transmission spectra of normally incident white light through the arrays of nanoholes presented in Figure 3. The peaks in Figure 3 at 637 nm (Figure 3a), 646 nm (Figure 3b), and 651 nm (Figure 3c) correspond to the extraordinary transmission mediated by SP excitation² (the experimental details for the transmission measurements can be found elsewhere¹¹).

For normally incident light into a 2D periodic square array of nanoholes, the SP resonance is dependent on the dielectric constant of the metal (ϵ_m), the dielectric properties of the metal–dielectric interface (ϵ_{eff}), and the distance between the center of the holes (periodicity, p), as described in eq 1:

$$\lambda^{\text{SP}}(i,j) = p(i^2 + j^2)^{-1/2} \left(\frac{\epsilon_{\text{eff}}\epsilon_m}{\epsilon_{\text{eff}} + \epsilon_m} \right)^{1/2} \quad (1)$$

where i and j are integers. The position of the wavelength of the maximum transmission is slightly red-shifted from

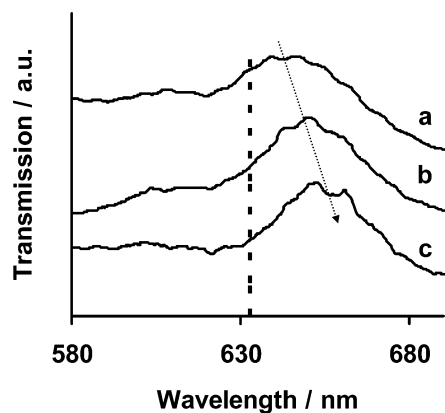


Figure 3. Transmission spectra of white light through three arrays of nanoholes with different periodicities (experimental setup described in ref 11). The periodicities were (a) 560 nm; (b) 590 nm; (c) 620 nm. The vertical dashed line shows the position of the laser excitation (632.8 nm). The dashed arrow helps to visualize the shift of the wavelength of maximum transmission with the periodicity. The spectra are offset for clarity.

this SP-resonance frequency. This equation neglects the perturbation of the SP modes, which leads to a slight redshift to the measured resonance frequency.^{7,21}

The dashed line in Figure 3 shows the wavelength of the laser used for Raman excitation (He–Ne, 632.8 nm). It can be seen in Figure 1 that the laser was transmitted through the nanoholes to the gold surface from the glass side. An increase in the amount of laser photons that reach the gold–air interface is expected when the wavelength of the laser light coincides with the enhanced transmission for normal incidence. The SP-resonance allows the creation of an extended enhanced field at the surface with the same frequency of the incident laser and tightly localized at the gold–air interface.^{22,23} The size of this near-field localization was calculated to be about 40 nm.²² Since the magnitude of the enhancement is related to this localized field, the strongest Raman signal is expected from molecules adsorbed on the array that have the resonant transmission closer to the laser frequency. This correlation between the enhancement of the Raman signal and the transmission spectra for different arrays was indeed observed in Figures 2 and 3.

Raman experiments involving other molecules adsorbed on the same arrays of nanoholes (the cleaning procedure for the arrays is presented elsewhere¹¹) were also attempted. The Raman spectra from both rhodamine 6G (R6G) and pyridine (py) adsorbed on the arrays of nanoholes showed a very low signal-to-noise ratio (not shown). One possible explanation for this is that these molecules may not adsorb as strongly to the metallic substrates as does oxa. However, good quality SERS from both R6G and py adsorbed on other types of SERS substrates (roughened electrode surface and colloids) are routinely reported,^{12,19} indicating that a monolayer of these molecules was probably adsorbed. Therefore, the lack of a strong Raman signal from adsorbed R6G and py (compared to oxa) in our experiments with arrays of nanoholes suggests that an internal electronic resonance is necessary (oxa has an absorption band centered around 620 nm). Blank experiments performed using oxa-coated glass

slides did not yield measurable Raman spectra. Attempts to obtain Raman signals in reflection mode from an oxa-coated, smooth gold surface also failed. These experiments show that the electronic resonance alone cannot explain the large Raman signal and their dependence on the periodicities of the nanoholes (Figure 2). Therefore, both the nanostructure and a resonance between the excitation and an internal molecular electronic transition are needed for the observation of increased Raman signal from oxa dye adsorbed on the arrays.

The magnitude of the spectroscopic response can provide some insights into the enhanced local electromagnetic field. Experiments involving nanoholes in gold coated with a monolayer of egg-white avidin labeled with Cy-5 dyes showed a 10× to 40× increase in the fluorescence efficiency (considering unity transmission through individual holes).^{16,18} An increase of 2 orders of magnitude in the IR absorption was also reported for 1-dodecanethiol adsorbed on Ni microarrays.¹⁷ Another study showed that optical nonlinear processes (second-harmonic generation) from a “bull’s-eye” structure involving a single nanohole in a thin silver film were enhanced by 4 orders of magnitude²⁴ (this corresponds to a 100× increase in the local electric field for this second-order process). These measurements are in good agreement with numerical calculations, using a differential method, which predicted a field enhancement of 2 orders of magnitude under resonance conditions.²²

In the context of plasmon-enhanced Raman scattering, the expected enhancement factor should be proportional to the product of the square of the local fields at both the excitation and the scattered frequencies.²⁵ This is because the SP resonances are relatively broad and are excited by both the incident and the Raman-shifted photons.²⁵ Therefore, an enhancement of 2 orders of magnitude in each field due to the extraordinary transmission would translate into an enhancement factor of 10⁴. Unfortunately, the absolute enhancement factor for oxa could not be experimentally determined, due to the high degree of fluorescence generated by the dye for this excitation wavelength. On the other hand, a relative enhancement factor of ca. 2 × 10⁵ was estimated for the 585 cm⁻¹ band in Figure 2a. In this case, the intensity of the ring-breathing mode of liquid benzene was used as a normal Raman standard. The relative enhancement factor calculated for Figure 2c is of the order of 10⁴. The SP-mediated enhancement and the resonance-Raman contributions are all included in these enhancement factors. We also estimate that the enhancement factor (relative to the benzene ring breathing) for py and R6G was lower than 10² (only SP-mediated enhancement were presented in these cases). It is important to emphasize, however, that these enhancement factors were calculated without considering the attenuation of the light field due to the sub-wavelength apertures. Only a small fraction of the excitation photons are able to travel through the sub-wavelength holes from the glass to the gold–air interface to actually excite the molecules (the transmitted laser power is as low as 1% of the laser power at the head). Experiments using the same arrangement as Figure 1, but with the incident excitation from

the Au–air side of the substrate (containing oxa) yielded Raman signals at least 1 order of magnitude smaller than those presented in Figure 2. Although the enhancement factor obtained here was smaller than generally observed from classical SERS substrates,¹² the array of nanoholes provides some advantages over those substrates. Among the advantages are the possibility to adjust the resonance through the periodicities to match a specific molecular target and the precise control over the spatial localization of the enhanced field.

In summary, this paper demonstrates enhanced-Raman scattering from molecules adsorbed on arrays of nanoholes in gold thin films. The intensity of the nanohole-enhanced Raman scattering was directly related to the periodicity of the arrays, confirming the role of SP resonances. The Raman spectra of oxa were further enhanced by coupling to internal electronic resonances from the adsorbed molecules as in the resonance-Raman effect. Good quality Raman scattering from nonresonant molecules that traditionally yield strong SERS, such as R6G and py, could not be observed. Thus, specific molecules can be distinguished by design of the nanohole array period, tuning the SP resonance to particular molecular electronic bands. Moreover, the mechanism of enhanced transmission through nanoholes involves the coupling between the SP modes from both sides of the metal–dielectric interfaces²³ (the side of the incident light and the side of the transmitted field). The SP coupling constant is maximized when a matching between the refractive index from the dielectric at both sides occurs. In a symmetric situation, where the dielectric constants of both sides are the same, the enhancement of the local field at the rims of the nanoholes is significantly increased.²³ It is then expected that nanohole-enhanced Raman scattering could be obtainable from molecules with no internal electronic transition in resonance with the laser excitation when a free-standing Au substrate is used. Moreover, the SP contribution to the overall Raman enhancement factor can be increased by using nanoholes in either silver or copper substrates, since these are known to produce a better SERS signals than gold.

The inelastic scattering from molecules adsorbed on nanoholes reported here is also useful for the design of practical applications. The vibrational information provided by Raman-labeled analytes is a molecular fingerprint, which renders a natural advantage for this method over SPR schemes for detection of biomolecules.²⁶ Methods for the preparation of cost-effective highly organized patterns of metallic nanostructures are available,²⁷ which opens the door for the fabrication of practical sensor chips for SERS. The enhanced Raman in transmission mode might be more convenient for detection systems in miniaturized devices,

although the backscattering geometry could still offer a better signal-to-noise ratio because it avoids the optical losses observed here for the transmission geometry.

Acknowledgment. We gratefully acknowledge funding support for this work from NSERC, CFI, and BCKDF. This collaboration has also been facilitated by the Centre for Advanced Materials and Related Technology (CAMTEC) at the University of Victoria and the Pacific Centre for Advanced Materials and Microstructures (PCAMM).

References

- (1) Raether, H. *Surface Plasmons on Smooth and Rough Surfaces and on Gratings*; Springer: Toronto, 1988.
- (2) Ebbesen, T. W.; Lezec, H. J.; Ghaemi, H. F.; Thio, T.; Wolff, P. A. *Nature* **1998**, *391*, 667–669.
- (3) Barnes, W. L.; Dereux, A.; Ebbesen, T. W. *Nature* **2003**, *424*, 824–830.
- (4) Altwischer, E.; Exter, M. P. v.; Woerdman, J. P. *Nature* **2002**, *418*, 304–306.
- (5) Srituravanich, W.; Fang, N.; Sun, C.; Luo, Q.; Zhang, X. *Nano Lett.* **2004**, *4*, 1085–1088.
- (6) Gordon, R.; Brolo, A. G.; McKinnon, A.; Rajora, A.; Leathem, B.; Kavanagh, K. L. *Phys. Rev. Lett.* **2004**, *92*, 037401.
- (7) Koerkamp, K. J. K.; Enoch, S.; Segerink, F. B.; Hulst, N. F. v.; Kuipers, L. *Phys. Rev. Lett.* **2004**, *92*, 183901.
- (8) Nice, E. C.; Catimel, B. *BioEssays* **1999**, *21*, 339–352.
- (9) Homola, J.; Yee, S. S.; Gauglitz, G. *Sens. Actuators B* **1999**, *54*, 3–15.
- (10) Jung, L. S.; Campbell, C. T.; Chinowsky, T. M.; Mar, M. N.; Yee, S. S. *Langmuir* **1998**, *14*, 5636–5648.
- (11) Brolo, A. G.; Gordon, R.; Leathem, B.; Kavanagh, K. L. *Langmuir* **2004**, *20*, 4813–4815.
- (12) Kneipp, K.; Kneipp, H.; Itzkan, I.; Dasari, R. R.; Feld, M. S. *Chem. Rev.* **1999**, *99*, 2957–2975.
- (13) Mulvaney, S. P.; He, L.; Natan, M. J.; Keating, C. D. *J. Raman Spectrosc.* **2003**, *34*, 163–171.
- (14) Duyn, R. P. v.; Hulst, J. C.; Treichel, D. A. *J. Chem. Phys.* **1993**, *99*, 2101–2115.
- (15) Brolo, A. G.; Irish, D. E.; Smith, B. D. *J. Mol. Struct.* **1997**, *405*, 29–44.
- (16) Liu, Y.; Blair, S. *Opt. Lett.* **2003**, *28*, 507–509.
- (17) Williams, S. M.; Stafford, A. D.; Rodriguez, K. R.; Rogers, T. M.; Coe, J. V. *J. Phys. Chem. B* **2003**, *107*, 11871–11879.
- (18) Liu, Y.; Bishop, J.; Williams, L.; Blair, S.; Herron, J. *Nanotechnology* **2004**, *15*, 1368–1374.
- (19) Brolo, A. G.; Sanderson, A. C.; Smith, A. P. *Phys. Rev. B* **2004**, *69*, 045424.
- (20) Brolo, A. G.; Sanderson, A. C. *Can. J. Chem.* **2004**, in press.
- (21) Genet, C.; Exter, M. P. v.; Woerdman, J. P. *Opt. Commun.* **2003**, *225*, 331–336.
- (22) Salomon, L.; Grillot, F.; Zayats, A. V.; Fornel, F. d. *Phys. Rev. Lett.* **2001**, *86*, 1110–1113.
- (23) Krishnan, A.; Thio, T.; Kim, T. J.; Lezec, H. J.; Ebbesen, T. W.; Wolff, P. A.; Pendry, J.; Martin-Moreno, L.; Garcia-Vidal, F. J. *Opt. Commun.* **2001**, *200*, 1–7.
- (24) Nahata, A.; Linke, R. A.; Ishi, T.; Ohashi, K. *Opt. Lett.* **2003**, *28*, 423–425.
- (25) Moskovits, M. *Rev. Mod. Phys.* **1985**, *57*, 783–826.
- (26) Cao, Y. C.; Jin, R.; Mirkin, C. A. *Science* **2002**, *297*, 1536–1540.
- (27) Murray, W. A.; Astilean, S.; Barnes, W. L. *Phys. Rev. B* **2004**, *69*, 165407.

NL048818W